The Effect of Molecular Weight on Passage of Proteins Through the Blood-Aqueous Barrier

Susanne Ragg,[1,2] Melissa Key,[3] Fernanda Rankin,[4] and Darrell WuDunn[5,6]

[1]Department of Pediatrics, University of Florida College of Medicine–Jacksonville, Jacksonville, Florida, United States
[2]Center for Computational Diagnostics, Department of Pediatrics, Indiana University School of Medicine, Indianapolis, Indiana, United States
[3]Department of Biostatistics, Fairbanks School of Public Health, Indiana University Purdue University Indianapolis, Indianapolis, Indiana, United States
[4]Department of Pediatrics, Indiana University School of Medicine, Indianapolis, Indiana, United States
[5]Department of Ophthalmology, University of Florida College of Medicine–Jacksonville, Jacksonville, Florida, United States
[6]Department of Ophthalmology, Glick Eye Institute, Indiana University School of Medicine, Indianapolis, Indiana, United States

Correspondence: Susanne Ragg, Department of Pediatrics, University of Florida College of Medicine–Jacksonville, 653-1 West 8th Street, LRC Fourth Floor, Jacksonville, FL 32209 USA;
susanne.ragg@jax.ufl.edu.

Submitted: January 1, 2019
Accepted: March 7, 2019

Citation: Ragg S, Key M, Rankin F, WuDunn D. The effect of molecular weight on passage of proteins through the blood-aqueous barrier. *Invest Ophthalmol Vis Sci*. 2019;60:1461–1469. https://doi.org/10.1167/iovs.19-26542

Purpose. To determine the effect of molecular weight (MW) on the concentration of plasma-derived proteins in aqueous humor and to estimate the plasma-derived and eye-derived fractions for each protein.

Methods. Aqueous humor and plasma samples were obtained during cataract surgery on an institutional review board–approved protocol. Protein concentrations were determined by ELISA and quantitative antibody microarrays. A total of 93 proteins were studied, with most proteins analyzed using 27 to 116 aqueous and 6 to 30 plasma samples.

Results. Plasma proteins without evidence of intraocular expression by sequence tags were used to fit a logarithmic model relating aqueous-plasma ratio (AH:PL) to MW. The log(AH:PL) appears to be well predicted by the log(MW) ($P < 0.0001$), with smaller proteins such as cystatin C (13 kDa) having a higher AH:PL (1:6) than larger proteins such as albumin (66 kDa, 1:300) and complement component 5 (188 kDa, 1:2500). The logarithmic model was used to calculate the eye-derived intraocular fraction (IOF) for each protein. Based on the IOF, 66 proteins could be categorized as plasma-derived (IOF<20), whereas 10 proteins were primarily derived from eye tissue (IOF >80), and 17 proteins had contribution from both plasma and eye tissue (IOF 20–80).

Conclusions. Protein concentration of plasma-derived proteins in aqueous is nonlinearly dependent on MW in favor of smaller proteins. Our study demonstrates that for proper interpretation of results, proteomic studies evaluating changes in aqueous humor protein levels should take into account the plasma and eye-derived fractions.

Keywords: aqueous humor, blood-aqueous barrier, proteins, plasma

Identification of the protein constituents of body fluid can lead to a better understanding of normal physiology and improve our understanding of the molecular underpinnings of common diseases. The aqueous proteome is of particular interest as it might be altered in many ocular diseases. Previous molecular analysis of the aqueous humor (AH) have mainly focused on the protein composition and the number of proteins in the Human Eye Proteome Project has increased to 827 proteins in 2018.[1]

To better understand the influence of the AH proteome on ocular physiology and disease, it is critical to differentiate between aqueous proteins derived from ocular structures and plasma-derived proteins that diffuse into AH. Although plasma-derived proteins may exert influence on ocular physiology, their levels within AH are highly dependent on their plasma levels. In contrast, proteins derived from intraocular structures are more likely to be internally regulated and hence are more likely to have direct impact on ocular function or be related to ocular pathophysiology.

In contrast to plasma, the AH is relatively free of proteins, so as to maintain clarity of vision. Plasma proteins are restricted from entering AH by the blood-aqueous barrier, although a significant portion of AH proteins originates from plasma. The blood-aqueous barrier is formed by the tight junctions of the nonpigmented epithelia of the ciliary body and posterior iris, and the nonfenestrated iris capillaries. Plasma proteins can pass through the fenestrated capillaries of the ciliary body but are prevented from entering the posterior chamber by the ciliary body nonpigmented epithelia. Similarly, plasma proteins circulating through iris capillaries are blocked from entering the iris stroma by the iris capillary vessel walls.[2,3]

However, plasma proteins that pass through the fenestrated capillaries of the ciliary body can diffuse through the ciliary body stroma into the iris stroma at the iris root. Because the anterior surface of the iris is not bound by any nonpenetrable barrier, plasma proteins within the iris stroma can then diffuse into the AH within the anterior chamber.[4,5]

According to Fick's laws of diffusion, small proteins diffuse through media more rapidly than large proteins. Thus, we

hypothesize a size-dependent relationship between the concentrations of proteins in AH relative to their plasma concentrations. A similar process has been described for plasma proteins entering the cerebrospinal fluid (CSF) through the blood-CSF barrier.[6,7] Previous proteomics studies on AH[8–18] have provided insight into the protein composition but to the best of our knowledge, a comprehensive analysis of the combined proteome of the AH and plasma has not yet been carried out. To test our hypothesis, we simultaneously determined the concentrations of 93 plasma proteins within plasma and AH and examined the effect of molecular weight (MW) on the ratio of AH concentration to plasma concentration.

We also introduce the eye-derived intraocular fraction (IOF) as an estimate of the proportion of each protein derived from ocular structures. This allows us to categorize the proteins into three groups: the proteins derived from the surrounding eye tissue, the proteins derived from the plasma, and proteins with contributions from both.

Methods

This study was approved by the Indiana University Institutional Review Board and followed the tenets of the Declaration of Helsinki. All subjects gave informed consent after explanation of the nature and possible consequences of the study.

Subjects

Aqueous samples were collected from eyes at the start of cataract surgery. Eligible subjects were older than 40, had no eye disease or disorder except cataract, had consented to undergo cataract surgery, and were willing to participate in this study. Exclusion criterion was prior intraocular surgery of any type, including laser.

Sample Collection and Clinical Data

AH samples were collected at the start of surgery by inserting a 30-gauge needle through the peripheral cornea and withdrawing approximately 100–250 μL of aqueous into a tuberculin syringe. Alternatively, a paracentesis was created with a 15-degree blade and the aqueous sample collected with a 30-gauge cannula on a tuberculin syringe. The aqueous sample was immediately transferred to a barcode-labeled cryotube, placed on ice, and transported to the Biospecimen Repository where the specimens were stored at −80°C until proteomic analysis. Clinical data and information associated with the AH sample were entered into the caTISSUE suite software that we have adapted for eye disease research.

Blood samples were collected in EDTA-coated vacutainers from a subset of subjects just before the start of surgery. To obtain platelet-poor plasma, a double spin protocol was used. Blood samples were first centrifuged at 3000*g* at room temperature for 10 minutes. The plasma was transferred to a sterile 2-mL Eppendorf tube without disturbing the buffy coat and subjected to a second centrifugation step at 12,000*g* for 10 minutes. The platelet-poor plasma was aliquoted into sterile cryovials and stored at −80°C. Samples were frozen within 2 hours of collection.

Enzyme-Linked Immunosorbent Assay

Protein concentration in aqueous and plasma samples was measured using commercial ELISA kits (Abcam, Cambridge, UK; Raybiotech, Norcross, GA, USA; LifeSpan BioScience, Seattle, WA, USA) as per the manufacturer's instruction. Standards, AH samples, and diluted plasma samples were added to 96-well plates containing highly purified protein-specific antibodies, incubated, and washed. Protein-specific biotinylated detection antibody was added, incubated, and washed, followed by the addition of an enzyme substrate, then a stop solution. Plates were read at 450 nm with a Tecan GENios Pro Multifunction Microplate Reader (Tecan, Mannedorf, Switzerland). Concentration estimates were found by fitting a four-parameter log-logistic model to a standard curve generated alongside the experimental data using the drc package[19] in R.[20]

Quantitative Antibody Microarray Analysis

The proteins in AH and plasma of patients were analyzed with the glass-slide quantitative antibody microarray platform (Quantibody; Raybiotech), which enables the accurate concentration determination of multiple proteins simultaneously. Proteins were combined in the same experiment based on their similar expected concentration range in AH and plasma. The proteins were screened for cross reactivity by the Raybiotech support staff. Antibodies to 20 to 40 proteins, along with positive and negative controls, were spotted onto a glass slide in quadruplicate. Samples were assayed according to the manufacturer's protocol.

Briefly, the glass slides were blocked, incubated with 70 μL of AH or plasma overnight at 4°C, washed, and then incubated with the biotin-conjugated antibodies specific for the proteins bound to the antibody on the glass slide. The slides were developed with streptavidin-labeled Cy3 equivalent dye and the signal was quantified using a laser scanner (GenePix 4000A; Molecular Devices Corporation, San Jose, CA, USA) at four different settings of the photomultiplier tube gain. These were combined using a linear regression model, in which the log-observed intensity at each spot was modeled as a function of gain for unsaturated spots with intensities at or above 200. Poor-quality spots were removed from the analysis based on visual inspection. Data were then normalized using the positive controls. Concentration estimates were found by fitting a four-parameter log-logistic model to a standard curve generated alongside the experimental data using the drc[19] package in R.[20]

Protein Data

The theoretical MW of a protein was calculated using the sequence of the circulating protein chain from the UniProt Knowledgebase[21,22] and the Compute pI/Mw tool of the ExPASy bioinformatic resource portal.[23] We conducted literature searches to identify the experimentally determined MW of the circulating form of each protein and the theoretical MW was adjusted when experimental data were available.

Statistical Analysis

For each protein, we modeled the concentration on the log scale using a mixed effects model with fluid (AH or plasma) as a predictor. Subjects were treated as random effects to incorporate correlation between fluids from the same patient. The variance was estimated separately for each fluid. From each analysis, we obtained the concentration ratio between aqueous and plasma (AH:PL), the standard errors associated with each estimate, and the correlation across the two fluids. All analyses were conducted using the nlme[24] and multcomp[25] packages in R.

To predict the diffusion component of AH proteins, we first selected a subset of high-abundance plasma proteins measured by ELISA with no evidence of intraocular expression by sequence tags (EST) within the ciliary body,[26] iris,[27] cornea,[28]

Investigative Ophthalmology & Visual Science

Table 1. Patient Demographics of Aqueous and Plasma Samples

	AH			Plasma			
	n	Age, Median (Min, Max)	% Male	*n*	Age, Median (Min, Max)	% Male	Proteins
Quantitative antibody microarray							
Group 1	116	68.9 (45.8, 94.6)	53.4	14	68.4 (55.5, 87.4)	57.1	35 proteins (see Table 2)
Group 2	27*	72.4 (54.2, 85.7)	48.1	6	66.4 (55.5, 80.1)	33.3	21 proteins (see Table 2)
ELISA							
Group 1	40	65.5 (48.6, 87.4)	50.0	24	67.1 (48.6, 87.4)	37.5	ALBU, ANGI, APOA1, APOA2, C05, C06, C07, C09, FINC, GELS, IgG, KNG1, TRFE
Group 2	40	68.9 (48.6, 87.4)	50.0	26	67.3 (48.6, 87.4)	46.2	A1AG, A2MG, AACT, AMBP, B2MG, CLUS, C03, C04, CYTC, DKK3, FETUA, HEMO, HPT, OSTP, RET4, TTHY, VTN
Group 3	30	65.2 (54.2, 82.8)	50.0	30	66.4 (53.6, 87.4)	70.0	FIB, CCL2
Group 4	40	68.9 (48.6, 87.4)	50.0	30	66.4 (53.6, 87.4)	70.0	CERU
Group 5	4	68.9 (45.8, 73.7)	25.0	4	71.0 (48.8, 76.3)	25.0	AFAM, A2GL
Group 6	5	65.1 (59.2, 71.3)	100.0	10	65.9 (48.6, 82.3)	40.0	APOC3
Group 7	12†	67.8 (55.5, 85.6)	40.0	10	73.3 (47.2, 94.1)	20.0	PEDF

* Quantitative antibody microarray group 2 was composed of six pooled AH samples, with three to six samples per pool.
† ELISA group 7 was composed of two pooled AH samples, with four and eight samples per pool.

anterior segment, trabecular meshwork,[29] lens,[30] retina,[31] and RPE/choroid[32] from the NEIBank sequence tag analysis project.[33–35] We then modeled AH:PL ratio, on the log scale as a function of the MW, also on a log scale:

$$\log_{10}(AH:PL) = a + b \times \log_{10}(\mathrm{MW}) + \epsilon$$

The data were fit using a weighted mixed effects model in which proteins were treated as random effects, and each protein ratio was weighted by its standard error using the metafor[36] package in R. Using this initial model, we calculated a 95% prediction interval for all proteins based on the MW.

To distinguish plasma-derived proteins from predominately eye-derived proteins, the IOF was calculated for each protein as

$$\mathrm{IOF} = \max\left(0, 1 - 10^{\text{upper bound} - \text{observed}}\right) \times 100,$$

as described by Reiber for CSF.[37,38] A final model was produced by also including proteins measured by quantitative antibody microarray that had an IOF of 0, no evidence of ESTs in ocular tissue, and minimal heterogeneity in the reported MW of the circulating plasma protein in the literature. This model was used to produce the final estimate of the IOF for all proteins.

Results

Samples were withdrawn from patients who ranged in age from 50 to 80. Table 1 shows the demographics of the AH and plasma samples used for the various protein analyses. Sample size for each protein measured is summarized in Table 2 for AH and plasma.

Analysis of AH Proteome by ELISA

To better understand the relationship between MW and AH concentration of plasma proteins, we sought to quantitate the concentrations of proteins that had been previously found by liquid chromatography tandem mass spectrometry in both aqueous[8–18] and plasma.[39–41] Forty proteins were selected based on the availability of high-sensitivity ELISA needed to detect the expected low concentration in AH. For 3 of the 40 proteins, the concentrations in AH were too low to be adequately quantified. The concentrations of proteins in AH versus plasma are shown in Figure 1. Relative to albumin, the primary protein component of both aqueous and plasma, low-MW proteins tend to be overrepresented in aqueous, whereas high-MW proteins tend to be underrepresented.

After determining the concentration of the 37 proteins, the ratio of AH concentration to plasma concentration (AH:PL) was calculated. As shown in Figure 2, smaller proteins such as cystatin C (CYTC, MW ~13 kDa) tend to have a higher AH:PL ratio (1:5.6) than larger proteins such as albumin (ALBU, MW ~66 kDa), which had an AH:PL ratio of 1:300, and complement component 5 (CO5, MW ~188 kDa), which had an AH:PL ratio of 1:2500. The plot of AH:PL versus MW is shown in Figure 2. The AH:PL of the 37 proteins is listed in Table 2.

Analysis of AH Proteome by Quantitative Antibody Microarray

To identify additional proteins that are quantifiable in aqueous, we screened 157 proteins by quantitative glass-slide antibody microarrays. Of the 157 proteins analyzed in initial screening assays, 101 proteins were not further studied: 42 proteins were not detectable in AH, 38 proteins were at the lower detection limit, and 21 proteins were in the linear range but were excluded for various reasons such as cross reactivity and plasma dilution requirements out of the range of the other proteins.

The remaining 56 proteins were further studied using larger sample sizes (up to 116 aqueous samples and 14 plasma samples) with quantitative antibody microarrays. Proteins were assigned to quantitative antibody microarray group 1 (Q1: 35 proteins) and group 2 (Q2: 21 proteins) based on dilution and protein cross reactivity. The concentration and AH:PLs of all 56 proteins measured by quantitative antibody microarray are included in Table 2.

Modeling AH:PL as Function of MW

Of the 37 proteins measured by ELISA, 17 that had no evidence of intraocular expression by EST were used to fit the model. Using this model, we calculated the IOF for all 93 proteins, which included the 37 proteins measured by ELISA and the 56 proteins measured by the quantitative antibody microarray (Table 2). Of the 56 proteins measured by quantitative antibody microarray, 10 proteins with an IOF of zero and no evidence of

Table 2. Protein Concentrations in AH and Plasma

			Aqueous Concentration		Plasma Concentration					
Protein Symbol	UniProt ID	MW, kDa	Mean (95% CI)	Units	Mean (95% CI)	Units	Ratio	IOF, %	Notes	ELISA Kit
ALBU	P02768	66	176 (168–185)	µg/mL	54 (49.4–58.9)	mg/mL	1:300	0	E1, M1	A
IGG		150	7.72 (7.52–7.92)	µg/mL	4.45 (4.32–4.58)	mg/mL	1:580	0	E1, M1	A
PEDF	P36955	50	6.23 (1.75–2.21)	µg/mL	6.14 (5.69–6.64)	µg/mL	1:1	96	E7	R
TTHY	P02766	55	6.13 (5.94–6.34)	µg/mL	305 (296–313)	µg/mL	1:50	0	E2	A
A1AG	P02763, P19652	43	5.31 (5.12–5.51)	µg/mL	1.21 (1.17–1.24)	mg/mL	1:230	0	E2, M1	A
TRFE	P02787	79.5	5.03 (4.94–5.11)	µg/mL	819 (805–834)	µg/mL	1:160	0	E1	A
HEMO	P02790	59	2.46 (2.39–2.54)	µg/mL	655 (646–664)	µg/mL	1:270	0	E2, M1	A
CERU	P00450	132	1.91 (1.75–2.08)	µg/mL	517 (507–527)	µg/mL	1:560	0	E4	A
A2MG	P01023	179	1.16 (0.98–1.37)	µg/mL	1.47 (1.43–1.5)	mg/mL	1:3500	0	E2	A
CYTC	P01034	13.34	961 (933–990)	ng/mL	5.39 (5.28–5.5)	µg/mL	1:5.6	0	E2	A
APOA1	P02647	56*	763 (730–797)	ng/mL	2.48 (2.41–2.56)	mg/mL	1:3300	0	E1	A
GELS	P06396	82.8	687 (650–725)	ng/mL	50.8 (49.4–52.1)	µg/mL	1:75	0	E1	L
AACT	P01011	57	623 (599–648)	ng/mL	220 (214–225)	µg/mL	1:350	0	E2	A
FETUA	P02765	59	476 (456–496)	ng/mL	240 (234–247)	µg/mL	1:510	0	E2, M1	R
VTNC	P04004	75	360 (348–374)	ng/mL	370 (363–377)	µg/mL	1:1000	0	E2, M1	R
DKK3	Q9UBP4	65	341 (330–353)	ng/mL	61.1 (59.7–62.5)	ng/mL	1:0.2	99	E2	R
CO3	P01024	185	245 (233–257)	ng/mL	814 (799–828)	µg/mL	1:3400	0	E2, M1	A
CLUS	P10909	80	233 (223–243)	ng/mL	68.1 (66.9–69.2)	µg/mL	1:290	0	E2	R
AMBP	P02760	26	210 (200–221)	ng/mL	88.6 (86.7–90.6)	µg/mL	1:430	0	E2, M1	A
CO4	P0C0L4,-5	210	187 (181–195)	ng/mL	210 (205–216)	µg/mL	1:1100	0	E2	A
B2MG	P61769	11.7	114 (111–118)	ng/mL	2.52 (2.47–2.58)	µg/mL	1:22	0	E2	A
RET4	P02753	75	89.6 (85.8–93.5)	ng/mL	33.6 (32.8–34.3)	µg/mL	1:380	0	E2	A
HPT	P00738	86*	78.5 (54.7–113)	ng/mL	603 (555–654)	µg/mL	1:5600	0	E2	A
CO9	P02748	71	60.8 (57.9–63.8)	ng/mL	60.9 (59.6–62.2)	µg/mL	1:1000	0	E1, M1	A
FIB	P02671,-5,-9	340	58.7 (53.8–64)	ng/mL	4.08 (3.97–4.19)	mg/mL	1:71000	0	E3, M1	A
OSTP	P10451	44	58.7 (55.6–61.9)	ng/mL	5.43 (5.32–5.54)	ng/mL	10.7:1	99	E2	R
CO7	P10643	110	58.2 (56–60.5)	ng/mL	53.3 (52.2–54.4)	µg/mL	1:920	0	E1, M1	A
CO6	P13671	108	57.7 (55.9–59.6)	ng/mL	78.5 (77.5–79.6)	µg/mL	1:1400	0	E1, M1	A
WIF1	Q9Y5W5	38.4	51.4 (39.1–67.5)	ng/mL	123 (71.5–211)	ng/mL	1:2.3	87	Q2	
FINC	P02751	550	45.6 (44.6–46.7)	ng/mL	241 (233–248)	µg/mL	1:5300	0	E1	A
AFAM	P43652	87	40.7 (23.3–71.3)	ng/mL	7.73 (6.6–9.05)	µg/mL	1:200	0	E5, M1	L
IBP6	P24592	32	34.3 (34.1–34.5)	ng/mL	631 (591–672)	ng/mL	1:20	0	Q1	
CO5	P01031	188	32.1 (31.1–33.2)	ng/mL	78.4 (77.3–79.5)	µg/mL	1:2400	0	E1, M1	A
APOA2	P02652	56*	22.5 (21.5–23.4)	ng/mL	30.8 (30.1–31.6)	µg/mL	1:1400	0	E1	A
KNG1	P01042	121	16.4 (15.8–17)	ng/mL	58.9 (57.7–60.2)	µg/mL	1:3600	0	E1, M1	A
APOC3	P02656	10.8	15.9 (11.3–22.3)	ng/mL	71.3 (60.9–83.4)	µg/mL	1:4500	0	E6	A
IBP2	P18065	31.4	11.1 (11–11.2)	ng/mL	206 (196–217)	ng/mL	1:18	0	Q1	
TIMP1	P01033	28	4.93 (4.88–4.98)	ng/mL	212 (194–233)	ng/mL	1:45	0	Q1	
VGFR1	P17948	110	4.64 (4.61–4.67)	ng/mL	12 (10.7–13.3)	ng/mL	1:2.5	98	Q1	
TIMP2	P16035	21.7	3.97 (3.54–4.44)	ng/mL	12 (10.9–13.2)	ng/mL	1:3	53	Q2	
ANGI	P03950	14	3.32 (3.26–3.39)	ng/mL	91.3 (89.4–93.3)	ng/mL	1:27	0	E1, M1	R
ICAM2	P13598	55	2.82 (2.79–2.85)	ng/mL	491 (395–611)	ng/mL	1:180	0	Q1, M2	
IBP3	P17936	150	2.66 (2.64–2.68)	ng/mL	927 (888–967)	ng/mL	1:350	0	Q1	
NCAM1	P13591	110*	2.59 (2.56–2.62)	ng/mL	491 (467–516)	ng/mL	1:190	0	Q1	
CD14	P08571	53	2.53 (2.51–2.55)	ng/mL	146 (137–155)	ng/mL	1:62	0	Q1	
IL6RB	P40189	100	2.35 (2.2–2.5)	ng/mL	77.1 (73.4–80.9)	ng/mL	1:33	64	Q2	
RARR2	Q99969	15.8	2.29 (1.81–2.89)	ng/mL	23.1 (13.8–38.8)	ng/mL	1:9.4	0	Q2, M2	
A2GL	P02750	55	1.96 (1.52–2.54)	ng/mL	1.9 (1.69–2.14)	µg/mL	1:980	0	E5, M1	L
MMP2	P08253	72	1.89 (1.85–1.93)	ng/mL	206 (171–247)	ng/mL	1:110	0	Q1	
TNF13	O75888	17	1.29 (1.27–1.32)	ng/mL	70.9 (64.8–77.5)	ng/mL	1:58	0	Q1	
CXL14	O95715	9.4	1.26 (1.24–1.27)	ng/mL	2.51 (2.32–2.7)	ng/mL	1:2.1	0	Q1	
TR11B	O00300	120	1080 (1070–1090)	pg/mL	597 (557–640)	pg/mL	1.8:1	99	Q1	
WFKN2	Q8TEU8	70	1.05 (1.04–1.06)	ng/mL	8.61 (8.19–9.04)	ng/mL	1:8.1	84	Q1	
CADH3	P22223	80	1040 (965–1120)	pg/mL	29.1 (26.1–32.5)	ng/mL	1:28	55	Q2	
TPO	P40225	70	802 (744–864)	pg/mL	11.5 (9.26–14.2)	ng/mL	1:14	72	Q2	
CXL16	Q9H2A7	35	779 (701–864)	pg/mL	6.64 (5.69–7.75)	ng/mL	1:8.5	43	Q2	
MMP3	P08254	57	671 (659–683)	pg/mL	46 (43.2–49)	ng/mL	1:67	0	Q1	
NOV	P48745	35.7	593 (589–597)	pg/mL	13.7 (12.9–14.6)	ng/mL	1:23	0	Q1	
CSF1R	P07333	85	502 (498–507)	pg/mL	634 (587–685)	ng/mL	1:1300	0	Q1	
C163A	Q86VB7	130	494 (490–499)	pg/mL	77.2 (72.8–81.8)	ng/mL	1:170	0	Q1	
CXCL6	P80162	8.3	452 (400–512)	pg/mL	4.37 (2.43–7.86)	ng/mL	1:9.2	0	Q2, M2	
ADAM9	Q13443	68	351 (299–412)	pg/mL	4.73 (1.91–11.7)	ng/mL	1:12	75	Q2	

Investigative Ophthalmology & Visual Science

Table 2. Continued

Protein Symbol	UniProt ID	MW, kDa	Aqueous Concentration Mean (95% CI)	Units	Plasma Concentration Mean (95% CI)	Units	Ratio	IOF, %	Notes	ELISA Kit
LEG3	P17931	31	340 (287–404)	pg/mL	7.64 (6.5–8.97)	ng/mL	1:23	0	Q2	
CCL2	P13500	8.6*	289 (282–297)	pg/mL	47.7 (46.7–48.7)	pg/mL	6.1:1	86	E3	A
VEGFA	P15692	45	286 (283–288)	pg/mL	1.53 (1.38–1.69)	ng/mL	1:5.4	76	Q1	
SPIT2	O43291	35	282 (240–332)	pg/mL	2.45 (1.8–3.36)	ng/mL	1:8.5	43	Q2	
INHBA	P08476	25	229 (216–242)	pg/mL	698 (644–757)	pg/mL	1:3	63	Q2	
SIGL9	Q9Y336	36	195 (174–219)	pg/mL	1.2 (0.947–1.52)	ng/mL	1:6.1	61	Q2	
VGFR2	P35968	160	179 (177–181)	pg/mL	8.22 (7.91–8.55)	ng/mL	1:46	77	Q1	
GPNMB	Q14956	115	159 (144–175)	pg/mL	9.87 (5.89–16.6)	ng/mL	1:57	50	Q2	
CATL1	P07711	41	156 (125–194)	pg/mL	2.53 (1.18–5.42)	ng/mL	1:14	30	Q2	
ANGP2	O15123	70	114 (113–115)	pg/mL	2.96 (2.77–3.16)	ng/mL	1:25	49	Q1	
PDGFA	P04085	28.9	97.6 (97.1–98.2)	pg/mL	4.57 (4.05–5.15)	ng/mL	1:44	0	Q1, M2	
KIT	P10721	98	94 (83.9–105)	pg/mL	35.6 (30.1–42.1)	ng/mL	1:380	0	Q2	
HGFL	P26927	78.4	93.5 (79.1–110)	pg/mL	4.8 (4.21–5.46)	ng/mL	1:52	14	Q2	
MIF	P14174	37.5	89.6 (88.6–90.7)	pg/mL	1.51 (1.35–1.69)	ng/mL	1:15	11	Q1	
MMP7	P09237	28	76.4 (75.4–77.4)	pg/mL	1.87 (1.67–2.11)	ng/mL	1:26	0	Q1, M2	
CXL10	P02778	8.6	69.7 (69–70.5)	pg/mL	378 (339–420)	pg/mL	1:4.8	0	Q1, M2	
TIE2	Q02763	75	68.8 (67.9–69.7)	pg/mL	2.73 (2.49–2.98)	ng/mL	1:41	26	Q1	
TR13B	O14836	13	68.4 (67.8–68.9)	pg/mL	1.87 (1.73–2.03)	ng/mL	1:29	0	Q1, M2	
GDF15	Q99988	30	57.9 (49.6–67.5)	pg/mL	1.16 (0.871–1.55)	ng/mL	1:20	0	Q2	
MMP10	P09238	57	57.2 (56.7–57.7)	pg/mL	121 (110–134)	pg/mL	1:2.3	93	Q1	
TNR1B	P20333	75	52.7 (52.1–53.3)	pg/mL	11.4 (10.5–12.3)	ng/mL	1:220	0	Q1, M2	
TNR1A	P19438	55	47 (46.6–47.3)	pg/mL	1.03 (0.947–1.12)	ng/mL	1:23	31	Q1	
MMP13	P45452	60	37.6 (37.3–37.8)	pg/mL	581 (552–612)	pg/mL	1:16	58	Q1	
HGF	P14210	80	33.9 (26–44.3)	pg/mL	215 (115–402)	pg/mL	1:6.1	90	Q2	
TNR16	P08138	42.5	28.9 (28.5–29.3)	pg/mL	1.02 (0.918–1.13)	ng/mL	1:36	0	Q1	
NTF4	P34130	28	28.5 (23.8–34)	pg/mL	501 (394–638)	pg/mL	1:18	0	Q2	
FGF7	P21781	28	12.9 (11.3–14.8)	pg/mL	147 (130–166)	pg/mL	1:11	0	Q2	
CCL11	P51671	8.4	10.4 (10.4–10.5)	pg/mL	269 (250–290)	pg/mL	1:27	0	Q1, M2	
FLT3L	P49771	21	10.2 (10.1–10.3)	pg/mL	213 (197–230)	pg/mL	1:21	0	Q1, M2	
UFO	P30530	80	5.72 (5.65–5.79)	pg/mL	210 (193–229)	pg/mL	1:38	39	Q1	
IL8	P10145	16	0.95 (0.94–0.95)	pg/mL	48.3 (42.8–54.6)	pg/mL	1:52	0	Q1	

A, Abcam; E1–E7, ELISA group 1–7; L, LSBio; M1, Model 1; M2, Model 2; Q1, Quantitative antibody microarray group 1; Q2, Quantitative antibody microarray group 2; R, Raybiotech.

* Lowest MW of multiple forms.

intraocular expression by ESTs were used to refine the model. The Notes column in Table 2 shows the proteins that were used to create (M1) and refine (M2) the model. The plot of AH:PL versus MW of all proteins is shown in Figure 2. Based on the IOF, the 93 proteins were categorized into three groups: proteins that are primarily derived from plasma (IOF <20; 66 proteins), proteins for which eye tissue is the principal source of synthesis (IOF >80; 10 proteins), and proteins with contribution from both eye tissue and plasma (IOF 20–80; 17 proteins). The data are shown in Figure 1 and summarized in Table 2.

The dependence of the IOF on MW is illustrated in Figure 2B for four proteins with a similar AH:PL ratio: C-X-C motif chemokine 14 (CXL14, 1:2.1), metalloproteinase inhibitor 2 (TIMP2, 1:3), Wnt inhibitory factor 1 (WIF1, 1:2.3), and vascular endothelial growth factor (VEGF) receptor 1 (VGFR1, 1:2.5). As the MW increases from 9 kDa for CXL14, to 22 kDa for TIMP2, to 38 kDa for WIF1, and to 110 kDa for VGFR1, the IOF increases from 0% for CXL14 to 53% for TIMP2, to 87% for WIF1 and to 98% for VGFR1. The data are shown in Figure 2 and summarized in Table 2.

Correlation Between Aqueous and Plasma Concentrations of Plasma-Derived Proteins

For aqueous and plasma samples that were obtained simultaneously from individual subjects, the correlation coefficient were estimated from the AH:PL ratio models for each protein.[42] Using those proteins derived from plasma with an IOF of zero, we found that low-MW proteins (less than 50 kDa) exhibited high correlation between aqueous and plasma concentrations. With increasing MW, the correlation between aqueous and plasma concentrations decreased to essentially zero for proteins with a MW of greater than 150 kDa (Fig. 3).

Rank Order of Proteins in AH Compared With Plasma

The concentration of individual proteins in the AH and plasma is listed in Table 2 in the order of decreasing concentration in AH. The examination of the rank order of the most abundant AH proteins shows that there is an order of magnitude difference between the most abundant protein, albumin, and the rest of the AH proteins. The fundamental difference in the rank order between aqueous and plasma is the relative increase of plasma-derived proteins with lower MW and the relatively high abundance of ocular-derived proteins in AH. This shift is highlighted in Table 3 for two examples of plasma-derived proteins with a relatively low MW, CYTC, and beta 2 microglobulin (B2MG). The three examples of ocular-derived proteins, pigment epithelium-derived factor (PEDF), Dickkopf-related protein 3 (DKK3), and osteopontin (OSTP), all with

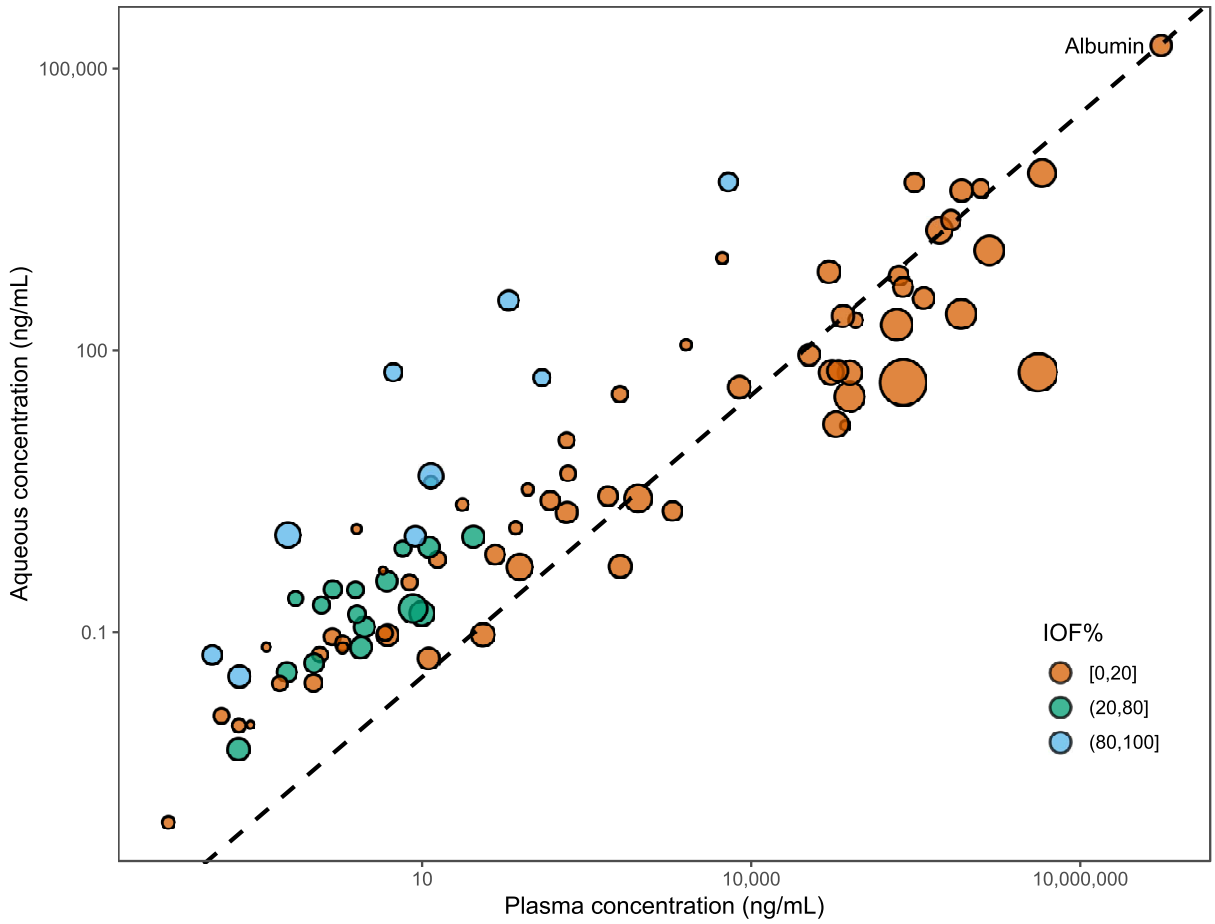

Figure 1. Effect of MW on the AH versus plasma protein concentration. The mean aqueous and plasma concentrations of 37 proteins as measured by ELISA are plotted. The area of the bubble represents the MW of the protein. The *dashed line* indicates the AH:PL of albumin (1:300). Proteins above the line are overrepresented (higher AH:PL) in AH relative to albumin, whereas proteins below the line are underrepresented (lower AH:PL) in AH relative to albumin. Proteins primarily derived from plasma are shown in *brown* (eye-derived IOF 0–20), proteins primarily derived from eye tissue are shown in *blue* (IOF 80–100), and proteins originating from both plasma and eye tissues are shown in *green* (IOF 20–80). Plasma-derived proteins smaller than albumin have a higher AH:PL than albumin (above the *dashed line*), whereas larger plasma-derived proteins have a lower AH:PL than albumin (below the *dashed line*).

IOF greater than 95%, highlight the relatively high contribution of proteins that are synthesized by ocular tissue.

The concept of the percent transfer, that is, how much of the total amount of plasma protein passes into AH (percent transfer = AH concentration / plasma concentration × 100), is shown in Table 3 for the four plasma-derived proteins.

Discussion

Although the protein component of AH is very dilute compared with that of plasma, most of the protein mass in AH is thought to arise from plasma. However, AH is not a simple diffusate of plasma, because it has both qualitative and quantitative differences in protein content relative to plasma.

By analyzing the MW of plasma-derived proteins in AH, we found that lower-MW proteins tended to penetrate AH more readily than higher-MW proteins. Indeed, AH concentrations of plasma-derived proteins are a function of MW. The logarithmic function is consistent with the model in which plasma proteins pass into AH by diffusing through ciliary body and iris stroma along a concentration gradient.[4,5,43] Our study adds to the mounting evidence that the blood-aqueous barrier, as it pertains to the anterior chamber, is best thought of as a size-dependent diffusional gradient.[4,5,43] A similar model has been proposed for entry of plasma proteins into CSF through the blood-CSF barrier.[6,7]

Introducing the AH:PL versus MW logarithmic function enables the estimation of the AH level of a plasma protein and the calculation of the contribution of intraocular tissues to the total aqueous concentration of the protein. By taking the IOF of an aqueous protein into account, one may be able to assess the protein's relative importance to ocular physiology and the pathogenesis of various eye diseases. Proteins with high IOF are more likely to be derived from the corneal endothelium, trabecular meshwork, iris, lens, and ciliary body, and represent disease biomarkers. These proteins may serve a potential target for further studies that look for differences in protein concentration in AH in various pathologic ocular conditions. In addition, our findings could be used to help understand what occurs in conditions associated with the breakdown of the blood-aqueous barrier. The most abundant proteins in AH, albumin and IgG, are plasma derived and have a low IOF. Although purely plasma-derived proteins may be important for normal ocular physiology, their aqueous concentrations are directly dependent on their plasma concentration and MW and thus their ocular function is regulated by their systemic levels.

It is important to note some limitations building our model. We assume that a protein is essentially plasma-derived if it is a known high-abundance plasma protein and lacks a known EST

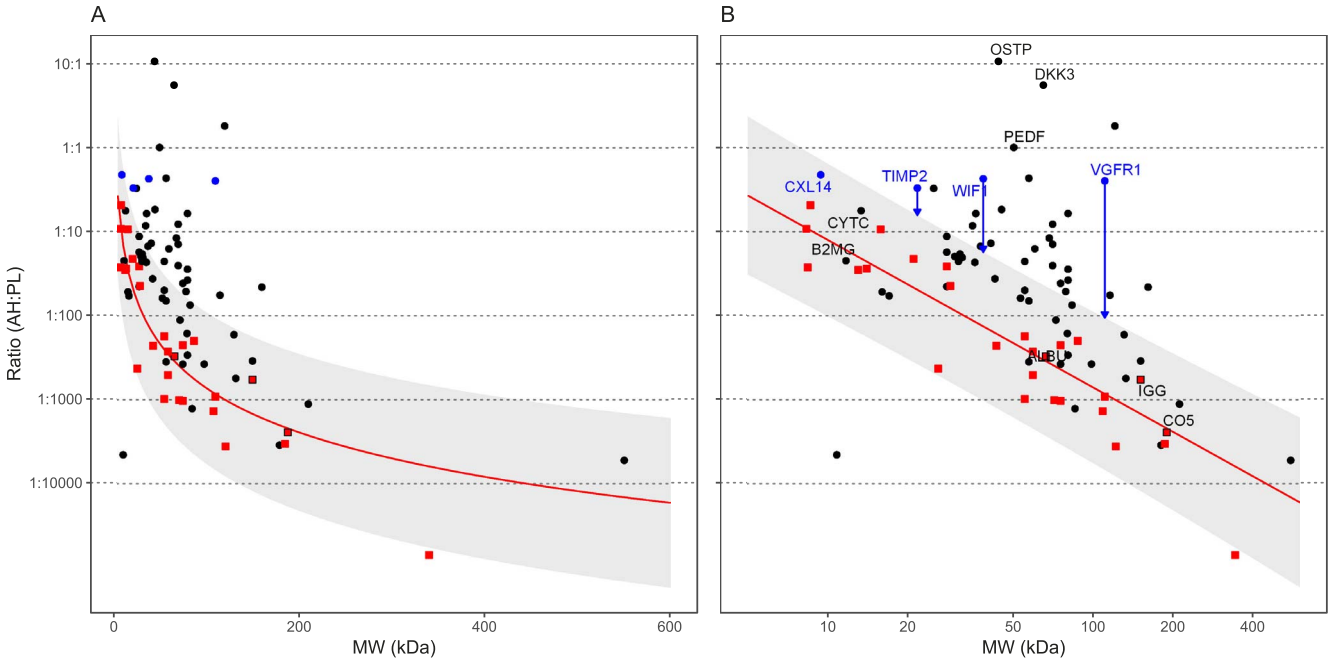

Figure 2. The AH:PL as a function of MW. The AH:PL ratio for 93 proteins measured in both fluids. Proteins represented by *red squares* were used to construct the model. Proteins represented by *blue circles* illustrate the dependence of the IOF on MW. The curve is logarithmic as a function of MW (**A**), and linear when plotting MW on a log scale (**B**). The shaded regions show the 95% prediction interval.

from intraocular tissues. The catalog of genes identified by EST sequencing of a cDNA library reflects a random sample of the mRNA present in the cell. For abundantly expressed genes, the library provides a good indication of the gene transcription in the tissue. However, less transcriptionally active genes might be missed during the generation of the library. Furthermore, transcript levels do not necessarily reflect protein levels.[44] Hence, we may have missed the intraocular contribution to the aqueous concentration for some low-abundance proteins. However, given the overall curve fitting, we think the intraocular contribution for the proteins used to build the model is likely negligible.

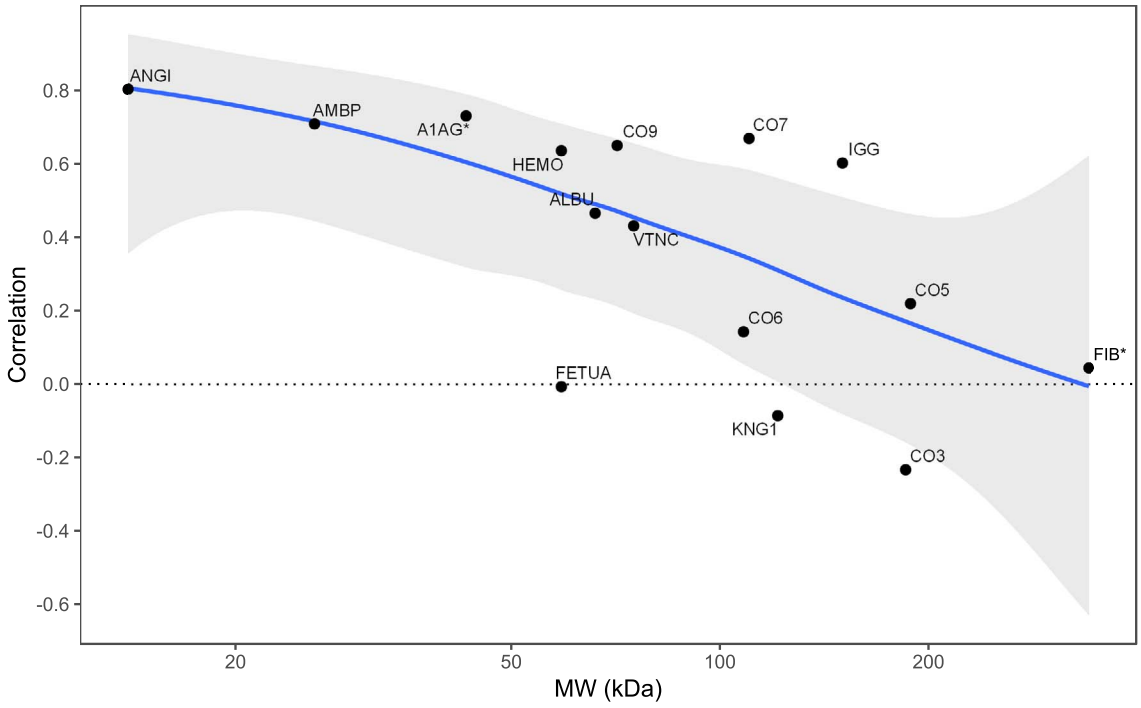

Figure 3. Correlation between AH and plasma as a function of MW. For plasma-derived proteins with no evidence of ocular production, the correlation between AH and plasma tends to be high when the MW is low (< 50 kDa), decreasing when the MW is between 50 and 150 kDa, and approximately 0 for MWs above 150 kDa. The *shaded region* gives a 95% confidence interval for the smoothed curve.

Table 3. Comparative Rank of Proteins in AH and Plasma

Protein	Rank in AH	Rank in Plasma	MW, kDa	IOF, %	Percent Transfer
ALB	1	1	60	0	0.3
IGG	2	2	150	0	0.17
PEDF	3	30	50	96	NA
CYTC	10	31	13	0	17
DKK3	16	49	65	99	NA
B2MG	21	32	12	0	4.5
OSTP	26	64	44	99	NA

NA, not applicable; Percent transfer = AH concentration / Plasma concentration × 100.

Another limitation of our targeted approach is that the analysis is restricted to proteins that are available for ELISA and/or quantitative antibody microarrays. Therefore, only a very limited number of proteins in AH could be quantified. Although our study was thorough, the 93 proteins we quantified in both the AH and plasma are only a fraction of the aqueous proteome.

Between aqueous and plasma samples collected concurrently, we found strong correlations in concentrations for small proteins but poor correlations for large proteins. This suggests that small proteins diffuse rapidly enough into AH to quantitatively reflect the plasma concentrations. In contrast, larger proteins diffuse far more slowly into AH so that by the time the proteins reach the AH, the plasma concentrations have changed sufficiently such that there is no longer correlation between the corresponding concentrations.

In conclusion, to our knowledge, this study is the first to simultaneously measure the protein concentration in aqueous and plasma in a large number of proteins. Our comprehensive analysis, demonstrating the logarithmic relationship of the MW and the AH:PL, enables an estimate of the contribution of intraocular tissues to the total aqueous concentration of a protein. Moreover, taking the IOF of proteins into account may help guide future studies of AH proteomics by providing potential ocular-derived protein targets that are relevant to ocular physiology and disease.

Acknowledgments

The authors thank the contributions of Louis B. Cantor, Yara Catoira-Boyle, Rudy Yung, and Shailaja Valluri for obtaining aqueous samples during cataract surgery.

Supported by the BrightFocus Foundation, Clarksburg, MD (SR), and the American Glaucoma Society, San Francisco, CA (DW).

Disclosure: **S. Ragg**, RayBIotech (F); **M. Key**, None; **F. Rankin**, None; **D. WuDunn**, None

References

1. Ahmad MT, Zhang P, Dufresne C, Ferrucci L, Semba RD. The Human Eye Proteome Project: updates on an emerging proteome. *Proteomics*. 2018;18:e1700394.
2. Bill A. The blood-aqueous barrier. *Trans Ophthalmol Soc U K*. 1986;105:149–155.
3. Raviola G. The structural basis of the blood-ocular barriers. *Exp Eye Res*. 1977;25:27–63.
4. Freddo TF. Shifting the paradigm of the blood-aqueous barrier. *Exp Eye Res*. 2001;73:581–592.
5. Freddo TF. A contemporary concept of the blood-aqueous barrier. *Prog Retin Eye Res*. 2013;32:181–195.
6. Reiber H. Proteins in cerebrospinal fluid and blood: barriers, CSF flow rate and source-related dynamics. *Restor Neurol Neurosci*. 2003;21:79–96.
7. Reiber H. Knowledge-base for interpretation of cerebrospinal fluid data patterns. Essentials in neurology and psychiatry. *Arq Neuropsiquiatr*. 2016;74:501–512.
8. Bennett KL, Funk M, Tschernutter M, et al. Proteomic analysis of human cataract aqueous humour: comparison of one-dimensional gel LCMS with two-dimensional LCMS of unlabelled and iTRAQ®-labelled specimens. *J Proteomics*. 2011;74:151–166.
9. Chowdhury UR, Madden BJ, Charlesworth MC, Fautsch MP. Proteome analysis of human aqueous humor. *Invest Ophthalmol Vis Sci*. 2010;51:4921–4931.
10. Anshu A, Price MO, Richardson MR, et al. Alterations in the aqueous humor proteome in patients with a glaucoma shunt device. *Mol Vis*. 2011;17:1891–1900.
11. Bouhenni RA, Al Shahwan S, Morales J, et al. Identification of differentially expressed proteins in the aqueous humor of primary congenital glaucoma. *Exp Eye Res*. 2011;92:67–75.
12. Duan X, Lu Q, Xue P, et al. Proteomic analysis of aqueous humor from patients with myopia. *Mol Vis*. 2008;14:370–377.
13. Kim TW, Kang JW, Ahn J, et al. Proteomic analysis of the aqueous humor in age-related macular degeneration (AMD) patients. *J Proteome Res*. 2012;11:4034–4043.
14. Richardson MR, Segu ZM, Price MO, et al. Alterations in the aqueous humor proteome in patients with Fuchs endothelial corneal dystrophy. *Mol Vis*. 2010;16:2376–2383.
15. Rosenfeld C, Price MO, Lai X, Witzmann FA, Price FW Jr. Distinctive and pervasive alterations in aqueous humor protein composition following different types of glaucoma surgery. *Mol Vis*. 2015;21:911–918.
16. Taube AB, Hardenborg E, Wetterhall M, et al. Proteins in aqueous humor from cataract patients with and without pseudoexfoliation syndrome. *Eur J Mass Spectrom (Chichester)*. 2012;18:531–541.
17. Murthy KR, Rajagopalan P, Pinto SM, et al. Proteomics of human aqueous humor. *OMICS*. 2015;19:283–293.
18. Pollreisz A, Funk M, Breitwieser FP, et al. Quantitative proteomics of aqueous and vitreous fluid from patients with idiopathic epiretinal membranes. *Exp Eye Res*. 2013;108:48–58.
19. Ritz C, Baty F, Streibig JC, Gerhard D. Dose-response analysis using R. *PLoS One*. 2015;10:1–13.
20. R Development Core Team. R: A language and environment for statistical computing (2008). R Foundation for Statistical Computing, Vienna, Austria. Available at: http://www.R-project.org.
21. Pundir S, Martin MJ, O'Donovan C. UniProt protein knowledgebase. *Methods Mol Biol*. 2017;1558:41–55.
22. The UniProt Consortium. UniProt: the universal protein knowledgebase. *Nucleic Acids Res*. 2017;45:D158–D169.
23. Artimo P, Jonnalagedda M, Arnold K, et al. ExPASy: SIB bioinformatics resource portal. *Nucleic Acids Res*. 2012;40:W597–W603.
24. Pinheiro J, Bates D, DebRoy S, Sarkar D. R Core Team. nlme: Linear and Nonlinear Mixed Effects Models (2018). R package version 3.1-137. Available at: https://CRAN.R-project.org/package=nlme.
25. Hothorn T, Bretz F, Westfall P. Simultaneous inference in general parametric models. *Biom J*. 2008;50:346–363.
26. Coca-Prados M, Escribano J, Ortego J. Differential gene expression in the human ciliary epithelium. *Prog Retin Eye Res*. 1999;18:403–429.
27. Wistow G, Bernstein SL, Ray S, et al. Expressed sequence tag analysis of adult human iris for the NEIBank Project: steroid-

response factors and similarities with retinal pigment epithelium. *Mol Vis*. 2002;8:185–195.

28. Rabinowitz YS, Dong L, Wistow G. Gene expression profile studies of human keratoconus cornea for NEIBank: a novel cornea-expressed gene and the absence of transcripts for aquaporin 5. *Invest Ophthalmol Vis Sci*. 2005;46:1239–1246.
29. Tomarev SI, Wistow G, Raymond V, Dubois S, Malyukova I. Gene expression profile of the human trabecular meshwork: NEIBank sequence tag analysis. *Invest Ophthalmol Vis Sci*. 2003;44:2588–2596.
30. Wistow G, Bernstein SL, Wyatt MK, et al. Expressed sequence tag analysis of adult human lens for the NEIBank Project: over 2000 non-redundant transcripts, novel genes and splice variants. *Mol Vis*. 2002;8:171–184.
31. Wistow G, Bernstein SL, Wyatt MK, et al. Expressed sequence tag analysis of human retina for the NEIBank Project: retbindin, an abundant, novel retinal cDNA and alternative splicing of other retina-preferred gene transcripts. *Mol Vis*. 2002;8:196–204.
32. Wistow G, Bernstein SL, Wyatt MK, et al. Expressed sequence tag analysis of human RPE/choroid for the NEIBank Project: over 6000 non-redundant transcripts, novel genes and splice variants. *Mol Vis*. 2002;8:205–220.
33. Wistow G. A project for ocular bioinformatics: NEIBank. *Mol Vis*. 2002;8:161–163.
34. Wistow G. The NEIBank project for ocular genomics: data-mining gene expression in human and rodent eye tissues. *Prog Retin Eye Res*. 2006;25:43–77.
35. Wistow G, Peterson K, Gao J, et al. NEIBank: genomics and bioinformatics resources for vision research. *Mol Vis*. 2008; 14:1327–1337.
36. Viechtbauer W. Conducting meta-analyses in R with the metafor package. *J Stat Softw*. 2010;36:1–48.
37. Reiber H. Flow rate of cerebrospinal fluid (CSF)–a concept common to normal blood-CSF barrier function and to dysfunction in neurological diseases. *J Neurol Sci*. 1994;122: 189–203.
38. Reiber H, Peter JB. Cerebrospinal fluid analysis: disease-related data patterns and evaluation programs. *J Neurol Sci*. 2001;184:101–122.
39. Farrah T, Deutsch EW, Omenn GS, et al. A high-confidence human plasma proteome reference set with estimated concentrations in PeptideAtlas. *Mol Cell Proteomics*. 2011; 10:M110.006353.
40. Haab BB, Geierstanger BH, Michailidis G, et al. Immunoassay and antibody microarray analysis of the HUPO Plasma Proteome Project reference specimens: systematic variation between sample types and calibration of mass spectrometry data. *Proteomics*. 2005;5:3278–3291.
41. Hortin GL, Sviridov D, Anderson NL. High-abundance polypeptides of the human plasma proteome comprising the top 4 logs of polypeptide abundance. *Clin Chem*. 2008; 54:1608–1616.
42. Chakraborty H, Helms RW, Sen PK, Cohen MS. Estimating correlation by using a general linear mixed model: evaluation of the relationship between the concentration of HIV-1 RNA in blood and semen. *Stat Med*. 2003;22:1457–1464.
43. Bert RJ, Caruthers SD, Jara H, et al. Demonstration of an anterior diffusional pathway for solutes in the normal human eye with high spatial resolution contrast-enhanced dynamic MR imaging. *Invest Ophthalmol Vis Sci*. 2006;47:5153–5162.
44. Maier T, Guell M, Serrano L. Correlation of mRNA and protein in complex biological samples. *FEBS Lett*. 2009;583:3966–3973.

Investigative Ophthalmology & Visual Science